Eur Spine J (2008) 17:1522–1530
DOI 10.1007/s00586-008-0775-x

ORIGINAL ARTICLE

Altered disc pressure profile after an osteoporotic vertebral fracture is a risk factor for adjacent vertebral body fracture

Michael N. Tzermiadianos · Susan M. Renner · Frank M. Phillips · Alexander G. Hadjipavlou · Michael R. Zindrick · Robert M. Havey · Michael Voronov · Avinash G. Patwardhan

Received: 29 October 2007 / Revised: 2 August 2008 / Accepted: 31 August 2008 / Published online: 16 September 2008

Abstract This study investigated the effect of endplate deformity after an osteoporotic vertebral fracture in increasing the risk for adjacent vertebral fractures. Eight human lower thoracic or thoracolumbar specimens, each consisting of five vertebrae were used. To selectively fracture one of the endplates of the middle VB of each specimen a void was created under the target endplate and the specimen was flexed and compressed until failure. The fractured vertebra was subjected to spinal extension under 150 N preload that restored the anterior wall height and vertebral kyphosis, while the fractured endplate remained significantly depressed. The VB was filled with cement to stabilize the fracture, after complete evacuation of its trabecular content to ensure similar cement distribution under both the endplates. Specimens were tested in flexion-extension under 400 N preload while pressure in the discs and strain at the anterior wall of the adjacent vertebrae were recorded. Disc pressure in the intact specimens increased during flexion by 26 ± 14%. After cementation, disc pressure increased during flexion by 15 ± 11% in the discs with un-fractured endplates, while decreased by 19 ± 26.7% in the discs with the fractured endplates. During flexion, the compressive strain at the anterior wall of the vertebra next to the fractured endplate increased by 94 ± 23% compared to intact status ($p < 0.05$), while it did not significantly change at the vertebra next to the un-fractured endplate (18.2 ± 7.1%, $p > 0.05$). Subsequent flexion with compression to failure resulted in adjacent fracture close to the fractured endplate in six specimens and in a non-adjacent fracture in one specimen, while one specimen had no adjacent fractures. Depression of the fractured endplate alters the pressure profile of the damaged disc resulting in increased compressive loading of the anterior wall of adjacent vertebra that predisposes it to wedge fracture. This data suggests that correction of endplate deformity may play a role in reducing the risk of adjacent fractures.

Keywords Osteoporosis · Compression fractures · Adjacent fractures · Cement augmentation · Biomechanics · Intervertebral disc

M. N. Tzermiadianos · R. M. Havey · A. G. Patwardhan (✉)
Department of Orthopaedic Surgery and Rehabilitation,
Loyola University Medical Center, 2160 S. First Avenue,
Maywood, IL 60153, USA
e-mail: apatwar@lumc.edu

M. N. Tzermiadianos · A. G. Hadjipavlou
University Hospital of Crete, Heraklion, Crete, Greece

S. M. Renner · R. M. Havey · M. Voronov · A. G. Patwardhan
Department of Veterans Affairs,
Edward Hines Jr. VA Hospital, Hines, IL, USA

F. M. Phillips
Rush University, Chicago, IL, USA

M. R. Zindrick
Hinsdale Orthopaedic Associates, Hinsdale, IL, USA

Introduction

The presence of an osteoporotic vertebral compression fracture (OVCF) increases the risk for subsequent vertebral fractures [27, 30, 38]. Lindsay et al. [27] reported an incidence of 11.5% of new vertebral fractures within 1 year following one previous OVCF, whereas this incidence was 24% in women with two or more fractures. Similarly, Ross et al. [38] reported that a single fracture increases the risk fivefold for new vertebral fractures, while the presence of two or more fractures increases the risk 12-fold. Silverman

et al. [42] reported that 58% of women with one or more fractures had adjacent fractures, supporting the high rate of adjacent fractures in the natural history of the disease. In a similar fashion, new vertebral fractures, especially at the adjacent vertebral bodies, have been reported after cement augmentation of an osteoporotic vertebral fracture [11, 13, 21, 22, 24, 45, 48–51].

The severity of vertebral collapse and the residual kyphotic deformity have been associated with the risk for subsequent vertebral fractures [9, 35, 46]. Kyphotic deformity shifts the center of gravity forward, resulting in increased forward bending moments, which are in turn compensated by a contraction of the posterior spinal muscles, resulting in an increased load within the kyphotic segment [37, 52]. Using anterior wall strain gauges, Kayanja et al. [17, 18] showed that after an experimentally induced osteoporotic fracture, the addition of flexion to axial compression increases the axial compressive loads at the adjacent vertebrae, supporting the role of residual kyphosis.

In vitro experiments have shown that damage to the vertebral body endplate reduces the pressure in the nucleus of the adjacent disc [1, 3, 4] and generates peaks of compressive stress in the annulus, usually posteriorly to the nucleus [1, 3]. Stress concentrations are affected by posture, and lordosis has been associated with intensified stress in the posterior anulus [3]. Furthermore, load distribution between the trabecular centrum of the vertebral body and the cortex is dependent on the properties of the intervertebral disc [20, 28]. Therefore, the altered mechanical properties of the intervertebral disc after an osteoporotic compression fracture with endplate depression are expected to change load distribution to the adjacent areas of the spine.

The purpose of this biomechanical study was to test the hypothesis that the altered pressure profile of the intervertebral disc after an osteoporotic vertebral fracture, even in the absence of kyphotic deformity, will alter load transmission to the adjacent vertebra and increase vertical loading of the anterior wall of adjacent vertebrae, predisposing them to wedge fracture.

Materials and methods

Specimens and experimental set-up

Eight fresh frozen human lower thoracic (T7–T11) or thoracolumbar (T10–L2) specimens each consisting of five vertebrae were used. The specimens were from five females and three males whose ages ranged from 56 to 82 years (average: 69 ± 8.5 years). Specimens were radiographically screened to exclude existing osteoporotic fractures, severe intervertebral space narrowing, bridging osteophytes and signs of vertebral metastasis. The specimens were thawed at room temperature (20°C) 24 h before testing. The paravertebral muscles were dissected, while keeping the discs, ligaments and posterior bony structures intact. The cephalad and caudal vertebrae of each specimen were anchored in cups using bone cement and pins.

The specimen was fixed to the testing apparatus at the caudal end and was free to move at the cephalad end. A moment was applied by controlling the flow of water into bags attached to 50-cm loading arms fixed to the cephalad vertebra. The long moment arm used to apply the moment loading resulted in nearly equal bending moments at each level. A six-axis load cell (Model MC3A-6-250, AMTI Inc., Newton, MA) was placed under the specimen to measure the applied loads and moments. The apparatus allowed for continuous cycling of the specimen between specified maximum moment endpoints in flexion and extension.

The motion of the cephalad vertebra of the specimen relative to the caudal one was measured using an optoelectronic motion measurement system (model 3020, Optotrak; Northen Digital, Waterloo, ON, Canada). In addition, biaxial angle sensors (model 902–45; Applied Geomechanics, Santa Cruz, CA) were mounted on the cephalad and caudal vertebrae to allow real time feedback for the optimization of the preload path. The spines were instrumented with pressure transducers (model 060S-1000, Precision Measurement Co., Ann Arbor, MI) in the nucleus of the discs above and below the middle vertebra. The pressure transducers were calibrated prior to the testing of each specimen using a pressure chamber. The anterior wall of the vertebral bodies adjacent to the middle vertebra were instrumented with single element strain gauges (FLA-2-11-3L, Sokki Kenkyujo, Tokio) to measure vertical (compressive) strain (Fig. 1).

The concept of the follower load was used to apply compressive preload; therefore, the preload was applied along a path that followed the curve of the spine [32]. An advantage of follower load application is that segmental bending moments and shear forces due to the preload application are minimized [33]. This allows a multi-segment thoracic spine specimen to support physiologic compressive preloads without constraining the motion of the vertebrae in the sagittal plane [44]. The preload was applied using bilateral loading cables attached to the cup holding the cephalad vertebra. The cables passed freely through guides anchored to the vertebrae adjacent to the target vertebra (Fig. 1). To avoid the creation of stress risers, the cable guide mounting technique did not violate the cortices of the vertebral bodies adjacent to the target vertebra. The cable guide mounts allowed anterior–posterior adjustments of the follower load path. The alignment of the preload path was optimized by adjusting the cable

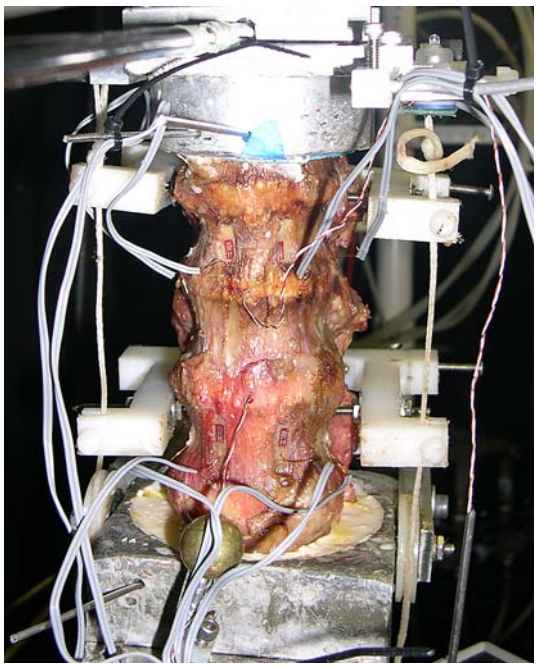

Fig. 1 Photograph of a specimen positioned on the testing apparatus. Strain gauges are mounted at the anterior walls and pressure sensors in the discs. Bilateral loading cables pass through guides mounted at the posterior elements

guide locations to minimize changes in the sagittal alignment of the specimen when compressive load up to 400 N was applied. The loading cables were connected to loading actuators under the specimen and were coated with radiopaque barium solution to be visible on X-ray images. A calibration marker (a radiopaque ball, 25.4 mm in diameter) was visible on each X-ray image.

Experimental protocol

Each specimen was first tested intact under flexion-extension moments (±6 Nm) with a 400 N compressive preload. Pressure was recorded at the discs above and below the middle vertebra and compressive strain was recorded at the anterior wall of the adjacent vertebrae. Total range of motion (ROM) of the specimen was measured using the optoelectronic motion measurement system.

Experimental creation of VCF

A novel technique was utilized to selectively fracture only one of the endplates of the middle VB of each specimen. Through a small opening on the anterior wall close to the target endplate, a void was created selectively under the endplate and was extended to one-third of the VB trabecular content; thereby creating a "stress-riser". (Fig. 2a, b). The endplate was carefully scraped free of trabecular connections using curettes and pituitaries. The void was randomly assigned under the upper endplate in four specimens and under the lower endplate in four. The specimen was flexed to 5 Nm and compressed using the loading cables until a fracture under the target endplate was observed on fluoroscopy or until a load limit of 700 N was reached (Fig. 2c). The maximum load limit of 700 N was used to avoid the likelihood of failure of the other endplate or other than the target vertebra; as this load magnitude is significantly less than the failure load reported in the literature [6, 7, 47]. If no fracture was observed on fluoroscopy, the instruments were reintroduced, the void was extended, and the specimen was again loaded in flexion and compression. After the fracture was established, the specimen remained under a physiologic compressive preload of 150 N. This value of compressive preload was selected taking into account the reported range of compressive preload on the lumbar spine in the prone position [39].

Reduction of the vertebral kyphotic deformity using spinal extension

The fracture was reduced by applying extension moment to the specimen under 150 N preload, aiming to completely

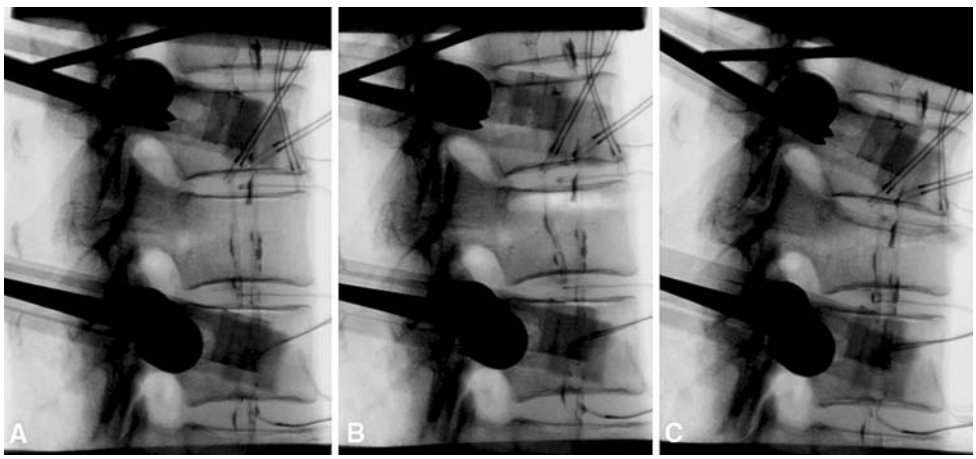

Fig. 2 Digital fluoroscopy images of a specimen. **a** Intact specimen. The bilateral loading cables, coated with radiopaque barium solution, are visible on the X-ray images. **b** Radiographic appearance of the void created under the upper endplate of the middle vertebra. **c** Image of the wedge fracture affecting only the upper part of the index vertebra

restore the pre-fracture anterior wall height and therefore correct the vertebral kyphosis angle (Fig. 3a). The extension moment was applied using upward force on the anterior loading arm fixed to the uppermost vertebra. After stabilization of the reduced fracture by cement injection into the void through the anterior opening, (Fig. 3b), the rest of the trabecular content in the middle VB was evacuated through a separate small anterior opening. The undamaged endplate was carefully scraped free of trabecular connections, and the rest of the VB was completely filled with cement under fluoroscopy to ensure proper cement distribution (Fig. 3c). Careful abrasion of both endplates ensured similar cement distribution near them. The specimen was then retested in flexion-extension (±6 Nm) under 400 N preload, and measurements of pressures at the discs adjacent to the middle vertebra and anterior wall compressive strains at the adjacent vertebrae were recorded.

Experimental creation of subsequent fractures

As a final step, the specimen was placed in flexion to 5 Nm and loaded in compression using the bilateral loading cables connected to actuators. The compressive load was gradually increased from 0 to 3,000 N or until a subsequent fracture was observed on fluoroscopy with a simultaneous sudden drop in the force versus time curve of the actuators.

Data analysis

The heights at the anterior wall and mid vertebral portion, as well as the vertebral kyphosis angle of the index vertebra were measured in the intact status, after the index fracture and after the reduction and augmentation. Mid vertebral height was measured using the depressed central endplate. Vertebral kyphosis angle was measured between the two end plates of the index vertebra. Measurements were performed on digital fluoroscopy images using computer software (Image Pro Plus, Media Cybernetics Inc). Flexion range of motion of the specimen was calculated as the angular change of the apical vertebra relative to the caudal one from the neutral posture to 6 Nm flexion. The force to failure for the index and the subsequent fractures was defined as the peak point of the force versus time curve.

The strain gauges used to measure anterior cortical strain were single element gauges and were connected in a quarter bridge (referring to Wheatstone bridge) configuration. In addition, the pressure sensors used to measure intervertebral disc pressure (model 060S) were quarter bridge diaphragm transducers. Strain gauges and transducers connected in a quarter bridge configuration are not capable of temperature compensation. These devices cannot be trusted to give absolute measurements since the output of the quarter bridge is a combination of thermal drift and measured value. Therefore, the disc pressure and adjacent vertebral wall compressive strain were normalized so that values in neutral position under 400 N preload were taken to zero, to compensate for thermal-drifting of sensors. As a result, the change in pressure and strain from neutral to full flexion before and after the creation and augmentation of the index fracture were used for analysis. Two specimens were excluded from pressure and strain analyses because of anterior slippage of pressure sensors during the experiment that resulted in inaccurate pressure recordings. The data were analyzed using repeated measures analysis of variance (ANOVA) with a significance level of $\alpha = 0.05$ using the commercial statistics package SPSS (SPSS Inc., Chicago, IL).

Results

In the intact specimens, vertebral kyphosis angle at the middle vertebra was 8.5 ± 2.2°, anterior wall height was 21.2 ± 2.7 mm, and mid vertebral height was

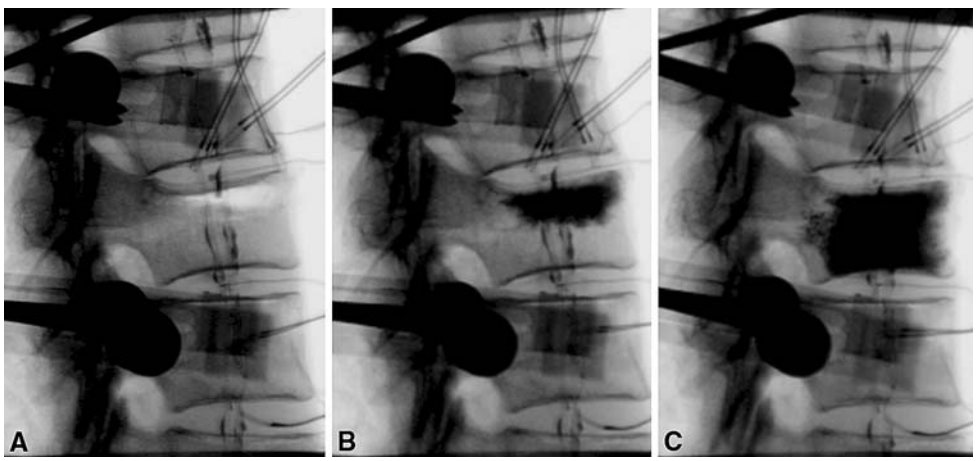

Fig. 3 Digital fluoroscopy images of a specimen **a** Reduction of anterior wall height and vertebral kyphosis angle with extension of the specimen while under 150 N preload. **b** Cement augmentation of the fracture. **c** Image showing the uniform distribution of cement under both endplates after careful abrasion of the un-fractured endplate

20.1 ± 2.9 mm. An average of 540 ± 150 N compressive load was required to fracture the target endplate of the index vertebra. No radiographic evidence of fractures at the non-target endplate or adjacent vertebral bodies was observed in any of the specimens. After the index fracture, vertebral kyphosis was 12.6 ± 2.4°, anterior wall height was 17.2 ± 3.1 mm and mid vertebral height was 14.3 ± 3.3 mm. A mean 4.6 ± 0.8 Nm extension moment, under 150 N preload, was sufficient to restore the kyphosis angle of the index vertebra to its intact value (8.8 ± 1.6°, $p = 0.38$). The anterior wall height was restored to 20.8 ± 2.6 mm, and the difference from the intact value, although statistically significant ($p = 0.04$), was small. Mid vertebral height remained significantly lower compared to intact (16.4 ± 3.0 mm, $p < 0.01$). Total flexion ROM of the specimens increased from 4.7 ± 1.4° in the intact status to 6.1 ± 2.4° after augmentation of the middle VB fracture. This increase was statistically significant ($p < 0.05$).

In the intact specimen, the pressure in the disc adjacent to the endplate assigned to remain un-fractured was 1.21 ± 1.82 MPa in the neutral posture under 400 N preload. Application of 6 Nm flexion moment increased disc pressure by 0.14 ± 0.11 MPa, representing an increase of 27.19 ± 17.4% from the pressure value in the neutral posture. After augmentation of the index fracture, the disc pressure in the neutral posture under 400 N preload was 1.34 ± 1.55 MPa. Application of 6 Nm flexion moment increased disc pressure by 0.13 ± 0.10 MPa, representing an increase of 15.8 ± 10.1% from the value in the neutral posture. The pressure change due to a flexion moment in the disc with undamaged endplates was not affected by the augmentation of the index fracture ($p = 0.55$). The disc pressure in the intact specimen adjacent to the endplate to be fractured was 0.51 ± 0.25 MPa in the neutral posture under preload. Application of 6 Nm flexion moment increased the pressure by 0.14 ± 0.10 MPa, representing an increase of 26.3 ± 9.5% from the pressure value in the neutral posture. After augmentation of the index fracture, the disc pressure at that level was 0.43 ± 0.13 MPa in the neutral posture under 400 N preload. Application of 6 Nm flexion decreased disc pressure by 0.07 ± 0.14 MPa, representing a decrease of 19.0 ± 26.8% from the value in the neutral posture (Fig. 4). The pressure change due to the application of the flexion moment in the disc with fractured endplate was significantly different from the intact ($p = 0.02$).

In the intact specimen, the compressive strain at the anterior wall of the VB adjacent to the endplate assigned to remain unfractured increased by 447.8 ± 100.4 microstrain due to the application of 6 Nm flexion moment as compared to the strain value in the neutral posture. After augmentation of the index fracture, the strain increased by 522.6 ± 131.5 microstrain from the neutral posture to 6 Nm flexion. (Fig. 4). This difference represents a non-significant change of 18.2 ± 7.1% in the anterior wall compressive strain of the adjacent vertebra next to the unfractured endplate, before and after the index fracture ($p > 0.05$). The strain at the anterior wall of the VB of the intact specimen adjacent to the endplate assigned for the index fracture increased by 413.2 ± 232.4 microstrain from the neutral posture to 6 Nm flexion. After augmentation of the index fracture, the strain increased by 836.2 ± 499.2 microstrain from the neutral posture to

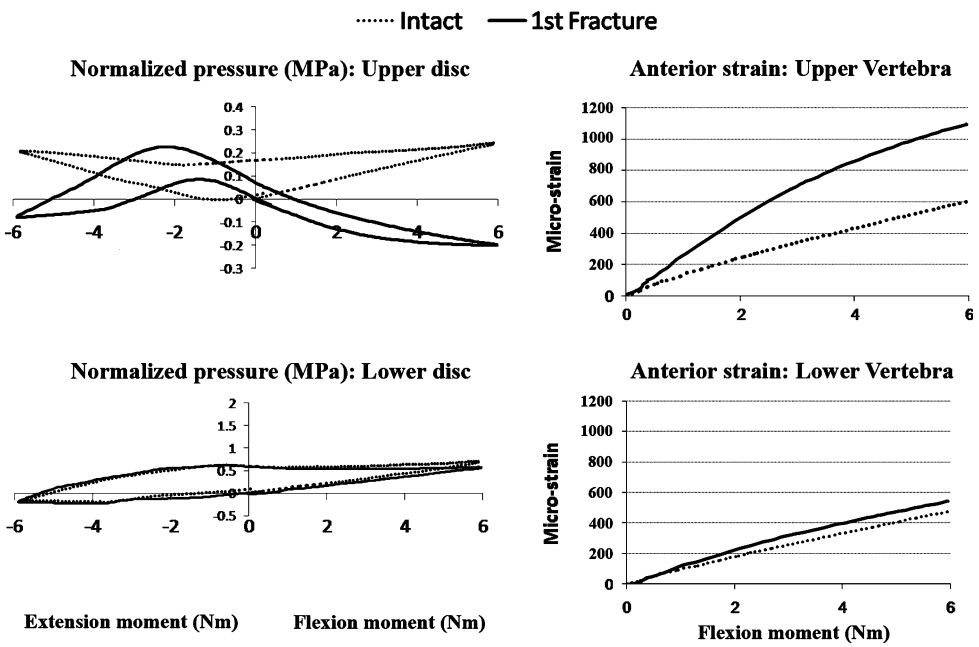

Fig. 4 Graphs showing the changes in the disc pressure (MPa) and anterior wall strain of the adjacent VBs (microstrain) after the selective damage to the upper endplate of the specimen shown in Figs. 2, 3. Data were collected during flexion-extension runs, under 400 N preload. Pressure and strain values were normalized so that values in neutral position under 400 N preload were taken to zero

6 Nm flexion. This difference represents a 94.2 ± 22.8% increase in the compressive strain of the anterior wall of the adjacent vertebra next to the damaged endplate, before and after the index fracture ($p < 0.05$). The maximum strain values seen in this study at 6 Nm of flexion were below 0.08% in all cases.

Subsequent compressive loading of the specimens in 5 Nm flexion resulted in a fracture of the adjacent VB close to the fractured endplate in six specimens and in a distal fracture at the uppermost VB in one specimen. Maximum load applied with the actuators failed to create a fracture in one of the specimens. The fractures of the adjacent vertebrae began as a depression in the anterior portion of the endplate (Fig. 5) that became gradually deeper as loading continued until the anterior wall finally failed. The failure load for the adjacent fractures was 1450 ± 402 N.

Discussion

This biomechanical study focused on the role of the endplate fracture as a risk factor for subsequent adjacent vertebral fractures. Cement was used only to stabilize the fracture and allow subsequent testing. The cementation technique used in this experiment is not relevant to any technique used in clinical practice. Because of the concerns existing in the literature about the presence of cement in the augmented vertebrae and how it may change their load bearing properties [5, 8, 34], both the endplates were carefully scraped free of any trabecular connections to ensure similar cement distribution underneath them. Therefore, any possible effect of cement presence under the endplates was a common denominator. Furthermore, restoration of the vertebral kyphosis angle by restoring the pre-fracture anterior wall height eliminated residual kyphosis as a risk factor for adjacent fractures leaving the endplate disruption as the only causal variable for the observed effects.

Experimental creation of a vertebral compression fracture is associated with uncertainty in both fracture pattern and location. Centrum defects have been previously used to assist in reproducing osteoporotic fractures in a target vertebra [12, 18]. The fracture model used in the current study allowed creating a predictable fracture not only at a target vertebra, but more specifically under the target endplate. The morphology of the fracture could also be controlled. The fracture began as depression of the weakened endplate and as the compressive load was increased, the anterior wall failed, progressing the fracture to a wedge shape while sparing the non-weakened endplate. In the current study, compressive loading was continued until the anterior wall height was reduced by approximately 25%.

Both in vivo [31, 39] and in vitro [4] studies have shown that in the intervertebral disc, the greatest pressures are exhibited in the forward flexed position under compression in activities such as lifting. The present study agrees with these findings. Furthermore, previous in vitro studies have documented that nuclear pressure is substantially reduced after an osteoporotic vertebral fracture [1, 2, 4, 10, 29] as more space becomes available for the nucleus. Our findings indicate a more specific impairment in the mechanical properties of the disc after endplate depression. The nucleus pressure is further decreased during flexion as compared to the already decreased value in the neutral posture reported in the literature. This abnormal mechanical behavior was accompanied with a simultaneous increase of the anterior wall compressive strain of the juxtaposed adjacent vertebra, which nearly doubled in

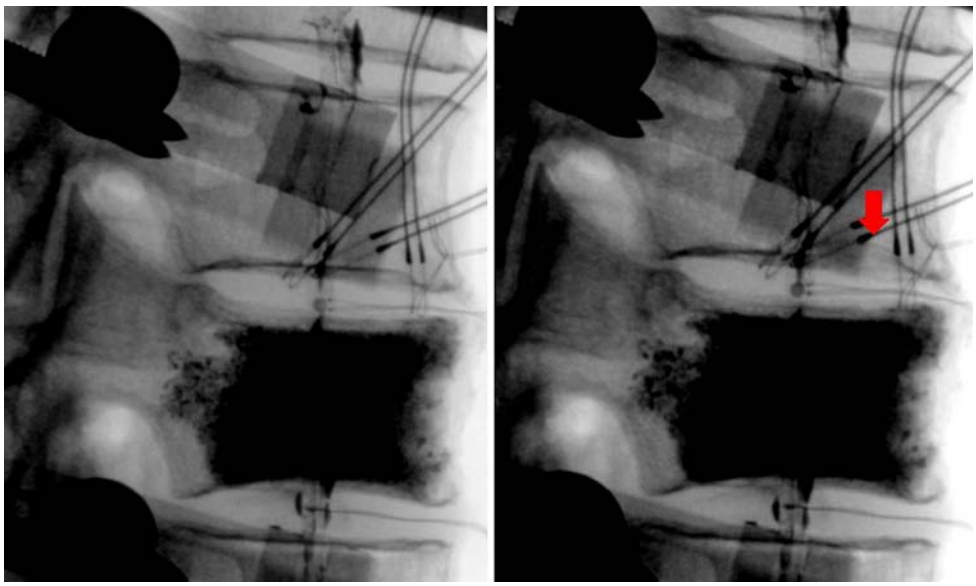

Fig. 5 Digital fluoroscopy images of the specimen shown in Figs. 2, 3 showing the initiation of a subsequent fracture at the anterior portion of the lower endplate of the upper adjacent vertebra (*arrow*), next to the damaged endplate of the index vertebra

flexion compared to the compressive stain in the intact status. On the contrary, the mechanical behavior of the undamaged disc of the fractured vertebra was not significantly affected and the compressive strain of the juxtaposed vertebral body was also not significantly altered. Previous investigators showed that anterior wall strain of adjacent vertebrae is increased with compressive load, but is more dramatically affected by flexion than by axial compression [15, 17, 18, 25, 36, 40]. Therefore, we can speculate that the small strain increase in the VB adjacent to the intact endplate found in this study could be explained by the increased flexion ROM that was observed after the fracture.

Cement augmentation using different surgical techniques, has been reported to only partially restore nucleus pressure, and the resultant pressure does not reach the pre-fracture condition [4, 10]. Our findings that after endplate fracture disc pressure is decreased during flexion as compared to the neutral posture are in contrast to previous experimental findings. Ananthakrishnan et al. [4] reported slightly higher disc pressure in flexion compared to the neutral position under axial compression after vertebroplasty for a VCF. In that study, pressure after vertebroplasty for an experimentally created vertebral fracture increased from 674 ± 111 kPa in the neutral posture under preload to 769 ± 165 kPa in the flexed position. This may suggest that the extension maneuver used in the present study to correct the vertebral kyphosis angle may have a detrimental effect on load transfer. Spinal extension exerts a ligamentotaxis effect through the anterior longitudinal ligament and annulus on the periphery of the fractured VB. Lacking tensile properties, the nucleus cannot exert a ligamentotaxis effect on the central part of the endplate, therefore central depression remains even after complete anterior wall reduction. In this context, elevation of the periphery of the endplate by spinal extension may enhance the relative central depression, leading to further compromise of nucleus mechanics. Clinical reports indicated that a greater degree of height restoration after vertebroplasty was associated with higher risk for new fractures [19, 26]. Similarly, another study reported that the rate of developing new symptomatic OVCFs after vertebroplasty was inversely correlated with the degree of wedge deformity of cemented vertebrae [23]. Although one might argue that higher cement volume in the less deformed vertebra may account for the increased rate of developing new fracture, those studies report that the risk of new fractures was not related to the volume of cement injected [23, 26]. Further clinical and biomechanical investigations are needed before reaching a definite conclusion.

It has been proposed that adjacent level load transfer through the vertebral centrum can be measured through adjacent disc pressure, while transfer through the vertebral shell can be measured through vertebral wall strain [4, 18]. Strain gauges bonded to the bone have been widely used to detect cortical bone deformation from load application. Surface strain distribution in the lumbar vertebrae measured by strain gauges has been shown to be directly proportional to compressive load [40]. Strain distribution, measured by surface strain gauges, has also been used as an indicator of the region where vertebral burst fracture initiates [15]. Similarly, stress concentration on the anterior cortex has been used to predict adjacent fracture risk after an osteoporotic compression fracture [17, 18]. Therefore, the findings from the current study support the hypothesis that endplate depression after fracture leads to significant reduction of load transfer through the centrum and increases adjacent level cortical strain, compensating for a lack of centrum support. The anterior shift of the load transfer path in flexion results in excessive load concentration in the anterior portion of the vertebra. After loading the cemented specimens to failure, nearly all subsequent fractures were located at the vertebra next to the damaged endplate. The fractures started as a depression of the anterior portion of the endplate close to the anterior wall, which subsequently led to anterior wall collapse as loading continued.

In vivo studies have reported that patients with degenerative discs have reduced nuclear pressure in all positions [39]. According to the hypothesis of the current study, those patients should also be at risk for osteoporotic vertebral fractures. This has been supported by a report that disc space narrowing is associated with an increased risk of vertebral fractures despite the higher BMD associated with spine osteoarthritis [43].

In conclusion, this study suggests that endplate depression after an osteoporotic vertebral fracture impairs the ability of the disc to distribute load evenly to the adjacent segments. Load concentration on the anterior portion of the adjacent vertebrae may contribute to increased subsequent fracture risk after an osteoporotic vertebral fracture. Current vertebral augmentation procedures for the treatment of osteoprotic VCFs have focused on the reduction of kyphosis angle and restoration of anterior vertebral body height with postural reduction or with the use of inflatable bone tamps [14, 16, 41]. The current study suggests that in addition to restoring spinal sagittal alignment, the ability to reduce the entire fractured endplate is important to restore load transmission across the fractured level.

Acknowledgments Institutional research support provided by the Department of Veterans Affairs, Washington, DC, and Kyphon Inc., Sunnyvale, CA.

References

1. Adams MA, McNally DS, Wagstaff J, Goodship AE (1993) Abnormal stress concentrations in lumbar intervertebral discs

following damage to the vertebral body: a cause of disc failure. Eur Spine J 1:214–221. doi:10.1007/BF00298362
2. Adams MA, McNally DS, Dolan P (1996) 'Stress' distributions inside intervertebral discs. The effects of age and degeneration. J Bone Joint Surg Br 78(6):965–972. doi:10.1302/0301-620X78B6.1287
3. Adams MA, Freeman BJ, Morrison HP, Nelson IW, Dolan P (2000) Mechanical initiation of intervertebral disc degeneration. Spine 25(13):1625–1636. doi:10.1097/00007632-200007010-00005
4. Ananthakrishnan D, Berven S, Deviren V et al (2005) The effect on anterior column loading due to different vertebral augmentation techniques. Clin Biomech (Bristol, Avon) 20:25–31. doi:10.1016/j.clinbiomech.2004.09.004
5. Baroud G, Nemes J, Heini P, Steffen T (2003) Load shift of the intervertebral disc after a vertebroplasty: a finite-element study. Eur Spine J 12(4):421–426. doi:10.1007/s00586-002-0512-9
6. Belkoff SM, Mathis JM, Deramond H et al (2001) An ex vivo biomechanical evaluation of hydroxyapatite cement for use with kyphoplasty. AJNR Am J Neuroradiol 22:1212–1216
7. Belkoff SM, Mathis JM, Fenton DC et al (2001) An ex vivo biomechanical evaluation of an inflatable bone tamp used in the treatment of compression fracture. Spine 26:151–156. doi:10.1097/00007632-200101150-00008
8. Berlemann U, Ferguson SJ, Nolte LP, Heini PF (2002) Adjacent vertebral failure after vertebroplasty: a biomechanical investigation. J Bone Joint Surg Br 84:748–752. doi:10.1302/0301-620X.84B5.11841
9. Black DM, Arden NK, Palermo L, Pearson J, Cummings SR (1999) Prevalent vertebral deformities predict hip fractures and new vertebral deformities but not wrist fractures. Study of Osteoporotic Fractures Research Group. J Bone Miner Res 14:821–828. doi:10.1359/jbmr.1999.14.5.821
10. Farooq N, Park JC, Pollintine P, Annesley-Williams DJ, Dolan P (2005) Can vertebroplasty restore normal load-bearing to fractured vertebrae? Spine 30(15):1723–1730. doi:10.1097/01.brs.0000171906.01906.07
11. Fribourg D, Tang C, Sra P, Delamarter R, Bae H (2004) Incidence of subsequent vertebral fracture after kyphoplasty. Spine 29(20):2270–2277. doi:10.1097/01.brs.0000142469.41565.2a
12. Gaitanis IN, Carandang G, Phillips FM, Magovern B, Ghanayem AJ, Voronov LI et al (2005) Restoring geometric and loading alignment of the thoracic spine with a vertebral compression fracture: effects of balloon (bone tamp) inflation and spinal extension. Spine J 5(1):45–54. doi:10.1016/j.spinee.2004.05.248
13. Grados F, Depriester C, Cayrolle G, Hardy N, Deramond H, Fardellone P (2000) Long-term observations of vertebral osteoporotic fractures treated by percutaneous vertebroplasty. Rheumatology 39:1410–1414. doi:10.1093/rheumatology/39.12.1410
14. Hadjipavlou AG, Tzermiadianos MN, Katonis PG, Szpalski M (2005) Percutaneous vertebroplasty and balloon kyphoplasty for the treatment of osteoporotic vertebral compression fractures and osteolytic tumours. J Bone Joint Surg Br 87(12):1595–1604. doi:10.1302/0301-620X.87B12.16074
15. Hongo M, Abe E, Shimada Y, Murai H, Ishikawa N, Sato K (1999) Surface strain distribution on thoracic and lumbar vertebrae under axial compression. Spine 24:1197–1202. doi:10.1097/00007632-199906150-00005
16. Hulme PA, Krebs J, Ferguson SJ, Berlemann U (2006) Vertebroplasty and kyphoplasty: a systematic review of 69 clinical studies. Spine 31(17):1983–2001. doi:10.1097/01.brs.0000229254.89952.6b
17. Kayanja MM, Ferrara LA, Lieberman IH (2004) Distribution of anterior cortical shear strain after a thoracic wedge compression fracture. Spine J 4(1):76–87. doi:10.1016/j.spinee.2003.07.003
18. Kayanja MM, Togawa D, Lieberman IH (2005) Biomechanical changes after the augmentation of experimental osteoporotic vertebral compression fractures in the cadaveric thoracic spine. Spine J 5(1):55–63. doi:10.1016/j.spinee.2004.08.005
19. Kim SH, Kang HS, Choi JA, Ahn JM (2004) Risk factors of new compression fractures in adjacent vertebrae after percutaneous vertebroplasty. Acta Radiol 45(4):440–445. doi:10.1080/02841850410005615
20. Kurowski P, Kubo A (1986) The relationship of degeneration of the intervertebral disc to mechanical loading conditions on lumbar vertebrae. Spine 11:726–731. doi:10.1097/00007632-198609000-00012
21. Lavelle WF, Cheney R (2006) Recurrent fracture after vertebral kyphoplasty. Spine J 6(5):488–493. doi:10.1016/j.spinee.2005.10.013
22. Ledlie JT, Renfro MB (2006) Kyphoplasty treatment of vertebral fractures: 2-year outcomes show sustained benefits. Spine 31(1):57–64. doi:10.1097/01.brs.0000192687.07392.f1
23. Lee WS, Sung KH, Jeong HT et al (2006) Risk factors of developing new symptomatic vertebral compression fractures after percutaneous vertebroplasty in osteoporotic patients. Eur Spine J 15(12):1777–1783. doi:10.1007/s00586-006-0151-7
24. Legroux-Gerot I, Lormeau C, Boutry N, Cotten A, Duquesnoy B, Cortet B (2004) Long-term follow-up of vertebral osteoporotic fractures treated by percutaneous vertebroplasty. Clin Rheumatol 23(4):310–317. doi:10.1007/s10067-004-0914-7
25. Lin HS, Liu YK, Adams KH (1978) Mechanical response of the lumbar intervertebral joint under physiological (complex) loading. J Bone Joint Surg 60(1):41–55
26. Lin CC, Chen IH, Yu TC, Chen A, Yen PS (2007) New symptomatic compression fracture after percutaneous vertebroplasty at the thoracolumbar junction. AJNR Am J Neuroradiol 28(6):1042–1045. doi:10.3174/ajnr.A0520
27. Lindsay R, Silverman SL, Cooper C et al (2001) Risk of new vertebral fracture in the year following a fracture. JAMA 285(3):320–323. doi:10.1001/jama.285.3.320
28. Liu L, Pei F, Song Y et al (2002) The influence of the intervertebral disc on stress distribution of the thoracolumbar vertebrae under destructive load. Chin J Traumatol 5:279–283
29. Luo J, Skrzypiec DM, Pollintine P, Adams MA, Annesley-Williams DJ, Dolan P (2007) Mechanical efficacy of vertebroplasty: influence of cement type, BMD, fracture severity, and disc degeneration. Bone 40(4):1110–1119. doi:10.1016/j.bone.2006.11.021
30. Melton LJ III, Atkinson EJ, Cooper C, O'Fallon WM, Riggs BL (1999) Vertebral fractures predict subsequent fractures. Osteoporos Int 10:214–221. doi:10.1007/s001980050218
31. Nachemson AL (1981) Disc pressure measurements. Spine 6(1):93–97. doi:10.1097/00007632-198101000-00020
32. Patwardhan AG, Havey RM, Meade KP, Lee B, Dunlap B (1999) A follower load increases the load-carrying capacity of the lumbar spine in compression. Spine 24:1003–1009. doi:10.1097/00007632-199905150-00014
33. Patwardhan AG, Havey RM, Carandang G, Simonds J, Voronov LI, Ghanayem AJ et al (2003) Effect of compressive follower preload on the flexion-extension response of the human lumbar spine. J Orthop Res 21:540–546. doi:10.1016/S0736-0266(02)00202-4
34. Polikeit A, Nolte LP, Ferguson SJ (2003) The effect of cement augmentation on the load transfer in an osteoporotic functional spinal unit, finite element analysis. Spine 28:991–996. doi:10.1097/00007632-200305150-00006
35. Pongchaiyakul C, Nguyen ND, Jones G et al (2005) Asymptomatic vertebral deformity as a major risk factor for subsequent fractures and mortality: a long-term prospective study. J Bone Miner Res 20(8):1349–1355. doi:10.1359/JBMR.050317

36. Ranu HS (1990) Measurement of pressures in the nucleus and within the annulus of the human spinal disc due to extreme loading. Proc Inst Mech Eng [H] 204:141–145. doi:10.1243/PIME_PROC_1990_204_248_02
37. Rohlmann A, Zander T, Bergmann G (2006) Spinal loads after osteoporotic vertebral fractures treated by vertebroplasty or kyphoplasty. Eur Spine J 15(8):1255–1264. doi:10.1007/s00586-005-0018-3
38. Ross PD, Genant HK, Davis JW, Miller PD, Wasnich RD (1993) Predicting vertebral fracture incidence from prevalent fractures and bone density among non-black, osteoporotic women. Osteoporos Int 3(3):120–126. doi:10.1007/BF01623272
39. Sato K, Kikuchi S, Yonezawa T (1999) In vivo intradiscal pressure measurement in healthy individuals and in patients with ongoing back problems. Spine 24(23):2468–2474. doi:10.1097/00007632-199912010-00008
40. Shah JS, Hampson WG, Jayson MI (1978) The distribution of surface strain in the cadaveric lumbar spine. J Bone Joint Surg 60-B(2):246–251
41. Shindle MK, Gardner MJ, Koob J, Bukata S, Cabin JA, Lane JM (2006) Vertebral height restoration in osteoporotic compression fractures: kyphoplasty balloon tamp is superior to postural correction alone. Osteoporos Int 17(12):1815–1819. doi:10.1007/s00198-006-0195-x
42. Silverman SL (1992) The clinical consequences of vertebral compression fractures. Bone 13(supp 1):261–267. doi:10.1016/8756-3282(92)90193-Z
43. Sornay-Rendu E, Munoz F, Duboeuf F, Delmas PD (2004) Disc space narrowing is associated with an increased vertebral fracture risk in postmenopausal women: the OFELY Study. J Bone Miner Res 19(12):1994–1999
44. Stanley SK, Ghanayem AJ, Voronov LI, Havey RM, Paxinos O, Carandang G et al (2004) Flexion-extension response of the thoracolumbar spine under compressive follower preload. Spine 29(22):E510–E514. doi:10.1097/01.brs.0000145417.94357.39
45. Tanigawa N, Komemushi A, Kariya S, Kojima H, Shomura Y, Sawada S (2006) Radiological follow-up of new compression fractures following percutaneous vertebroplasty. Cardiovasc Intervent Radiol 29(1):92–96. doi:10.1007/s00270-005-0097-x
46. The European Prospective Osteoporosis Study (EPOS) Group (2003) Determinants of the size of incident vertebral deformities in European men and women in the sixth to ninth decades of age: the European Prospective Osteoporosis Study (EPOS). J Bone Miner Res 18:1664–1673. doi:10.1359/jbmr.2003.18.9.1664
47. Tomita S, Kin A, Yazu M, Abe M (2003) Biomechanical evaluation of kyphoplasty and vertebroplasty with calcium phosphate cement in a simulated osteoporotic compression fracture. J Orthop Sci 8:192–197. doi:10.1007/s007760300032
48. Trout AT, Kallmes DF, Kaufmann TJ (2006) New fractures after vertebroplasty: adjacent fractures occur significantly sooner. AJNR Am J Neuroradiol 27(1):217–223
49. Trout AT, Kallmes DF, Layton KF, Thielen KR, Hentz JG (2006) Vertebral endplate fractures: an indicator of the abnormal forces generated in the spine after vertebroplasty. J Bone Miner Res 21(11):1797–1802. doi:10.1359/jbmr.060723
50. Uppin A, Hirsch J, Centenera L, Pfiefer B, Pazianos A, Choi I (2003) Occurrence of new vertebral fracture after percutaneous vertebroplasty in patients with osteoporosis. Radiology 226:119–124. doi:10.1148/radiol.2261011911
51. Voormolen MH, Lohle PN, Juttmann JR et al (2006) The risk of new osteoporotic vertebral compression fractures in the year after percutaneous vertebroplasty. J Vasc Interv Radiol 17(1):71–76
52. Yuan H, Brown C, Phillips FM (2004) Osteoporotic spinal deformity: a biomechanical rationale for the clinical consequences and treatment of vertebral body compression fractures. J Spinal Disord 17:236–242. doi:10.1097/00024720-200406000-00012